

# Synthesis of $\beta$ "-Alumina from Powder Mixtures Using Thermal Plasma Processing

Osamu Fukumasa, Satoshi Sakiyama and Hirotoishi Esaki

*Department of Electrical and Electronic Engineering,*

*Faculty of Engineering, Yamaguchi University,*

*2-16-1 Tokiwadai, Ube 755-8611, Japan*

With the use of a thermal plasma reactor based on the forced constricted type plasma jet generator, the synthesis of thermoelectric materials ( $\beta$ "-alumina) for the alkali metal thermoelectric converter (AMTEC) has been studied. Under not only atmospheric pressure but also low pressure, thin films of  $\beta$ "-alumina are successfully synthesized for the first time from powder mixtures of  $\alpha$ - $\text{Al}_2\text{O}_3$ ,  $\text{Na}_2\text{CO}_3$  and  $\text{MgO}$ . The powder mixing ratio, jet power and substrate position strongly affect the synthesis of  $\beta$ "-alumina, which is found to be correlated with jet temperature.

**KEYWORDS:** thermal plasma processing, plasma jet, synthesis of new ceramics, alkali metal thermoelectric converter (AMTEC),  $\beta$ "-alumina

## 1. Introduction

Thermal plasma processing using a plasma jet with high speed and high heat capacity under reduced pressure ( $\leq 100$  Torr) is one of the most promising methods for synthesizing new materials. To this end, we have developed a thermal plasma reactor<sup>1)</sup> composed of a forced constricted type plasma jet generator with a feed ring, and confirmed that this reactor generates stable plasma jets with a high heat capacity under various operating conditions<sup>2,3)</sup>. So far, we have carried out a performance test of the reactor in the production of ultrafine particles and spray coatings of refractory materials<sup>2,3)</sup>, as well as in the synthesis of diamonds<sup>4,5)</sup>. The typical deposition rate of spray coating with this system is about  $5 \mu\text{m/s}$  and that of diamond films is  $5\text{-}6 \mu\text{m/min}$ . These deposition rates are higher than those of other methods by two or three orders of magnitude.

The alkali metal thermoelectric converter (AMTEC), which utilizes sodium ions which conduct  $\beta$ "-alumina solid electrolyte, is a device that directly converts heat energy to electric energy<sup>6,7)</sup>. Because of its merits (high conversion efficiencies, high power densities, no moving parts and so on), the AMTEC is one of the most promising candidates for dispersed small-scale power stations, remote power stations and aerospace power systems. The AMTEC cell consists of a  $\beta$ "-alumina solid electrolyte and a metal electrode. According to theoretical considerations of the internal resistance and also to the results of experiments on a disk-type cell (where the film metal electrode was fabricated with a magnetron sputtering system)<sup>8)</sup>, the largest internal resistance was found to be governed by the resistance of  $\beta$ "-alumina.

In general, it is necessary to reduce the thickness of the  $\beta$ "-alumina layer to improve the generating power densities. However,  $\beta$ "-alumina is prepared by sintering and the film thickness has not been sufficiently decreased to optimize the AMTEC. It is also necessary to develop more porous thin film metal electrodes with lower resistivity to achieve a smooth flow of sodium gas. Therefore, the key issue for improving the performance characteristics of the AMTEC is how to fabricate plane-type  $\beta$ "-alumina thin films with both high electrical and low thermal conductivities and a porous molybdenum electrode with low resistance.

In this study, we aim at developing an integrated fabrication process for the AMTEC electrode, i.e., the preparation of  $\beta''$ -alumina solid electrolyte-molybdenum thin films by plasma spraying. According to our recent experimental results<sup>9)</sup>, the characteristics of thin films prepared by plasma spraying depends strongly on the operating pressure and dense films without pores are obtained under a low pressure. We expect that  $\beta''$ - alumina would be synthesized from powder mixtures and dense and thin  $\beta''$ -alumina coatings would be prepared successively by low-pressure plasma spraying. On the other hand, a porous molybdenum electrode is expected to be prepared under atmospheric pressure.

With the use of thermal plasma processing, we synthesized  $\beta''$ -alumina for the first time from powder mixtures of  $\alpha$ - $\text{Al}_2\text{O}_3$ ,  $\text{Na}_2\text{CO}_3$  and  $\text{MgO}$ <sup>10,11)</sup>, although the components of  $\beta$ -alumina were included in the prepared films. As the material for AMTEC,  $\beta''$ -alumina is more desirable because of its high ion conductivity compared with  $\beta$ -alumina, although both  $\beta$  and  $\beta''$ -alumina have sodium ions which conduct solid electrolytes.

We examined the following two subjects concerning the production and control of  $\beta''$ -alumina thin films:

- (1) Synthesis of  $\beta''$ -alumina films from powder mixtures
- (2) Characterization of prepared materials for use in AMTEC.

Here, we mainly report recent results concerning the synthesis of  $\beta''$ -alumina from powder mixtures and its dependence on experimental conditions.

## 2. Experimental Apparatus and Methods

A schematic diagram of the experimental setup is shown in Fig.1. The reactor is divided into three parts: the forced constricted type (FC-type) plasma jet generator, the feed ring (FR) and the vacuum vessel (processing region)<sup>2,3)</sup>. The FC-type plasma jet generator is composed of a nozzle anode, a rod cathode and an insulated constrictor nozzle (floating electrode). The nozzle anode (5 mm diameter, 4.5 mm length) is made of copper and the rod cathode (5 mm diameter) is of 2 % Th-

W. As we have reported elsewhere<sup>2,3</sup>, this reactor produces stable plasma jets with a high heat capacity not only under atmospheric pressure but also under reduced pressure.

Powder materials were injected into the plasma with carrier gas through two capillary feeding ports of the FR. For the synthesis of  $\beta$ -alumina, powder mixtures of  $\alpha$ -Al<sub>2</sub>O<sub>3</sub> and Na<sub>2</sub>CO<sub>3</sub> were used. For the synthesis of  $\beta''$ -alumina, it was necessary to add MgO to these powder mixtures.

Experiments were conducted under the following conditions: pressure ( $p'$ ) in the reaction chamber was varied from 20 to 760 Torr; working gas (Ar) flow rate was 20 l/min; carrier gas (Ar) flow rate was 6 l/min; powder flow rate was 0.5 g/min; net arc input power, i.e., jet power  $W_j$ , was maintained at 3 kW or 6 kW.

### 3. Experimental Results and Discussion

In thermal plasma processing, the injected powder materials should be completely melted or evaporated. Namely, the interaction between powder particles and plasma flow, i.e., the heat transfer from plasmas to particles, is important. The melting points of  $\alpha$ -Al<sub>2</sub>O<sub>3</sub>, Na<sub>2</sub>CO<sub>3</sub> and MgO are 2040 °C, 852 °C and 2800 °C, respectively. Thus, the preparation of  $\beta''$ -alumina may be more difficult than that of  $\beta$ -alumina because of the large difference in the melting points of the powder materials.

The synthesis of  $\beta$ -alumina was attempted before  $\beta''$ -alumina synthesis, using powder mixtures of  $\alpha$ -Al<sub>2</sub>O<sub>3</sub> and Na<sub>2</sub>CO<sub>3</sub>. According to the X-ray diffraction patterns of prepared thin films for various powder mixtures (see Fig.2), it is found that  $\beta$ -alumina can be successfully synthesized not only under atmospheric pressure but also under reduced pressure, and that the optimum percentage composition of Na<sub>2</sub>CO<sub>3</sub> ranges from 10 to 20 percent, where  $W_j = 3$  kW.

Next, we tested the synthesis of  $\beta''$ -alumina using powder mixtures to which MgO was added as the third material, because MgO plays an important role in stabilizing  $\beta''$ -alumina chemically. The effect of MgO on  $\beta''$ -alumina synthesis is studied as a function of the percentage composition of MgO. A typical example of the X-ray diffraction patterns of the synthesized film is shown in Fig.3.

Without MgO, only peaks of  $\beta$ -alumina are observed among the peaks of raw powder materials. When the percentage composition of the MgO is increased, peaks of  $\beta$ "-alumina appear and their intensities increase. When the percentage composition of the MgO is higher than 15%, however, the intensities conversely decrease. It suggests that  $\beta$ "-alumina is synthesized from powder mixtures of  $\alpha$ -Al<sub>2</sub>O<sub>3</sub>, Na<sub>2</sub>CO<sub>3</sub> and MgO, and there is an optimum percentage composition of MgO for synthesizing  $\beta$ "-alumina.

As far as we know,  $\beta$ "-alumina films prepared in this experiment are the first ones prepared by thermal plasma processing, although  $\beta$ -alumina is included. Also, there are some peaks of raw powder materials, i.e., peaks of  $\alpha$ -Al<sub>2</sub>O<sub>3</sub>, Na<sub>2</sub>CO<sub>3</sub> and MgO, in the X-ray diffraction patterns of the prepared films. To obtain a high thermoelectric conversion efficiency, pure  $\beta$ "-alumina films must be synthesized. To optimize the processing conditions, we studied the effects of the jet power  $W_j$ , the chamber pressure  $p_c$  and the distance  $L$  between the feed ring exit and the substrate on the synthesis of  $\beta$  and  $\beta$ "-alumina films.

According to the results of separate experiments<sup>2,9)</sup>, with decreasing chamber pressure  $p_c$ , the plasma jet increases in size in both axial and radial directions. Correspondingly, the high-temperature region and the high-velocity region expand. For example, the plasma volume at 100 Torr, where the temperature of the plasma jet is higher than the melting point of  $\alpha$ -Al<sub>2</sub>O<sub>3</sub>, is about 4.4 times that at 760 Torr, and the velocity of the plasma jet at  $L = 50$  mm increases from about 100 m/s to 530 m/s<sup>2)</sup>. Figure 4 shows the axial distributions of the plasma jet temperature at two different pressures, 760 Torr and 100 Torr. As is clearly shown, with increasing  $W_j$  or decreasing  $p_c$ , the high-temperature region shifts to the downstream region.

Figure 5 shows the X-ray diffraction patterns of the synthesized films as a function of  $L$  at  $p_c = 100$  Torr. In the downstream region where  $L$  is greater than 70 mm, a small peak of  $\beta$ "-alumina is observed among the many peaks of the raw powder materials. On the other hand, in the upstream region where  $L$  is less than 60 mm, many  $\beta$ "-alumina peaks appear distinctly and their intensities

increase markedly with decreasing  $L$ . At the same time, the raw material peaks become smaller. At  $L = 50$  mm,  $\beta''$ -alumina peaks become dominant, although small  $\beta$ -alumina and small MgO peaks are observed, but not Mo peaks, i.e., the substrate material. It is suggested that pure  $\beta''$ -alumina films are well synthesized in the upstream region of the plasma jet, i.e., the high-temperature region of the plasma jet. On the other hand, under atmospheric pressure, we have confirmed the same tendency that  $\beta$  and  $\beta''$ -alumina films are well synthesized with decreasing  $L$ . The optimum value of  $L$  is less than 30 mm.

Figure 6 shows typical SEM images of the deposited film at  $L = 80$  mm and 40 mm under  $p_r = 100$  Torr. According to the X-ray diffraction patterns shown in Fig.5,  $\beta$  and  $\beta''$ -alumina are synthesized more successfully in Fig.6(b). The film in Fig.6(a) is composed of particles with diameter less than  $10 \mu\text{m}$ , which are not well melted, and the film is porous. On the other hand, the film in Fig.6(b) is dense as the deposited powders are well melted.

Taking into account the results shown in Figs.4 and 5 and the discussion described above, there should be a strong correlation between the jet temperature and the synthesis of  $\beta''$ -alumina films. Though the axial jet temperature is nonuniform at each gas pressure, the temperature in the region where  $\beta''$ -alumina films are well synthesized is nearly the same regardless of pressure. Namely, the value is nearly equal to  $2400^\circ\text{C}$ , regardless of  $p_r$ .

Figures 7 and 8 show the effects of  $W_j$  and the species rate of powder mixtures of  $\alpha$ - $\text{Al}_2\text{O}_3$  and  $\text{Na}_2\text{CO}_3$  on  $\beta''$ -alumina synthesis, respectively. With increasing  $W_j$  (see Figs.7(a) and 7(b)), the peaks of raw materials decrease and the peaks of  $\beta$  and  $\beta''$ -alumina increase in number and amplitude as the jet temperature rises. With an increase in the percentage composition of  $\text{Na}_2\text{CO}_3$  (see Fig.8), the amplitudes of the peaks of  $\beta''$ -alumina increase markedly, reach a maximum and then decrease. The melting points of  $\text{Na}_2\text{CO}_3$  ( $852^\circ\text{C}$ ) and MgO ( $2800^\circ\text{C}$ ) are quite different. For  $\beta''$ -alumina synthesis, more sodium ions should be included in the prepared films than in  $\beta$ -alumina films. To this end, at least MgO (i.e., the stabilizer of sodium ions) should be well melted in front of

the substrate. Thus,  $\beta$ "-alumina is well synthesized in a high-temperature region (above 2400°C) of the plasma jet, and the optimum percentage composition of  $\text{Na}_2\text{CO}_3$  also depends on the plasma jet temperature (or  $L$  and  $W_j$ ).

The performance characteristics of the AMTEC strongly depend on two physical constants of the  $\beta$ "-alumina films, i.e., the thermal and electrical conductivities. In the preparation of  $\beta$ "-alumina,  $W_j$ ,  $L$  and the percentage composition of powder mixtures have been found to be the key parameters, which are correlated with the plasma jet temperature and heat transfer from plasmas to particles. Optimization of the processing conditions under which  $\beta$ "-alumina films with required physical constants are prepared is now under study.

#### 4. Conclusions

In order to clarify the application feasibility of a plasma jet reactor to the fabrication process of thermoelectric materials, we have attempted to synthesize  $\beta$ "-alumina films. In this study,  $\beta$ "-alumina films have been successfully synthesized for the first time from powder mixtures of  $\alpha$ - $\text{Al}_2\text{O}_3$ ,  $\text{Na}_2\text{CO}_3$  and  $\text{MgO}$ , using thermal plasma processing. There is a strong correlation between the temperature of the plasma jet and the synthesis of  $\beta$ "-alumina films. As the jet temperature increases,  $\beta$ "-aluminas predominate in the prepared thin films compared with  $\beta$ -alumina. Though pure  $\beta$ "-alumina films have not yet been synthesized, these experimental results lead us to suggest that pure  $\beta$ "-alumina synthesis could be realized by optimizing a combination of jet power, substrate position and mixing ratio of powder mixtures. The optimization of process conditions and the characterization of the prepared thin films for AMTEC have to be studied further.

#### Acknowledgement

A part of this work is supported by a Grant-in-Aid for Developmental Scientific Research from The Japanese Ministry of Education, Science, Sports and Culture.

## References

- 1) S. Saeki, O. Fukumasa and K. Osaki: Proc. 8th Int. Symp. Plasma Chemistry **3** (1987) 1989.
- 2) O. Fukumasa and S. Sakiyama: Trans. IEE Jpn. **112A** (1992) 269. (in Japanese)
- 3) S. Sakiyama, T. Hirabaru and O. Fukumasa: Rev. Sci. Instrum. **63** (1992) 2408.
- 4) S. Sakiyama, O. Fukumasa and K. Aoki: Jpn. J. Appl. Phys. **33** (1994) 4409.
- 5) S. Sakiyama, O. Fukumasa, T. Murakami and T. Kobayashi: Jpn. J. Appl. Phys. **36** (1997) 5003.
- 6) T. Cole: Science **221** (1983) 915.
- 7) T. Masuda: Ceramics **25** (1990) 609. (in Japanese)
- 8) T. Masuda, A. Negishi, K. Tanaka and T. Honda: Trans. IEE Jpn. **110B** (1990) 147.  
(in Japanese)
- 9) O. Fukumasa, S. Sakiyama and K. Osaki: Proc. The Japan-China Bilateral Symp. Advanced Materials Engineering "Novel Methods for Preparation and Evaluation of Coatings" (1999) p.58.
- 10) O. Fukumasa, S. Sakiyama and A. Nishida: Proc. 12th Symp. Plasma Processing (1995) p.549.
- 11) O. Fukumasa, S. Sakiyama, Y. Shirai and K. Hatano: Proc. 13th Symp. Plasma Processing (1996) p.157.



## Figure Captions

Fig.1. Schematic diagram of the plasma jet reactor system.

Fig.2. X-ray diffraction patterns of the prepared thin films at different concentrations of  $\text{Na}_2\text{CO}_3$ . Experimental conditions are: jet power  $W_j = 3$  kW and chamber pressure  $p_t = 760$  Torr.

Fig.3. X-ray diffraction patterns of the thin films as a function of MgO. Experimental conditions are:  $W_j = 3$  kW,  $p_t = 400$  Torr, and powder mixtures are  $\alpha\text{-Al}_2\text{O}_3(85\%)+\text{Na}_2\text{CO}_3(15\%)+\text{MgO}$ .

Fig.4. Axial distributions of the plasma jet temperature in the downstream region for two different pressures  $p_t = 100$  and  $760$  Torr.

Fig.5. X-ray diffraction patterns of the thin films as a function of  $L$ . Experimental conditions are:  $W_j = 3$  kW,  $p_t = 100$  Torr, and powder mixtures are  $\alpha\text{-Al}_2\text{O}_3(77\%)+\text{Na}_2\text{CO}_3(14\%)+\text{MgO}(9\%)$ .

Fig.6. SEM images of the prepared thin films. Experimental conditions are:  $W_j = 3$  kW,  $p_t = 100$  Torr, and powder mixtures are  $\alpha\text{-Al}_2\text{O}_3(77\%)+\text{Na}_2\text{CO}_3(14\%)+\text{MgO}(9\%)$ .

Fig.7. X-ray diffraction patterns of the prepared thin films at different jet powers. Experimental conditions are:  $p_t = 760$  Torr,  $L = 30$  mm, and powder mixtures are  $\alpha\text{-Al}_2\text{O}_3(77\%)+\text{Na}_2\text{CO}_3(14\%)+\text{MgO}(9\%)$ .

Fig.8. X-ray diffraction patterns of the thin films at different concentrations of  $\text{Na}_2\text{CO}_3$  and thus  $\alpha\text{-Al}_2\text{O}_3$ . Experimental conditions are:  $W_j = 6$  kW,  $p_t = 760$  Torr and  $L = 35$  mm.

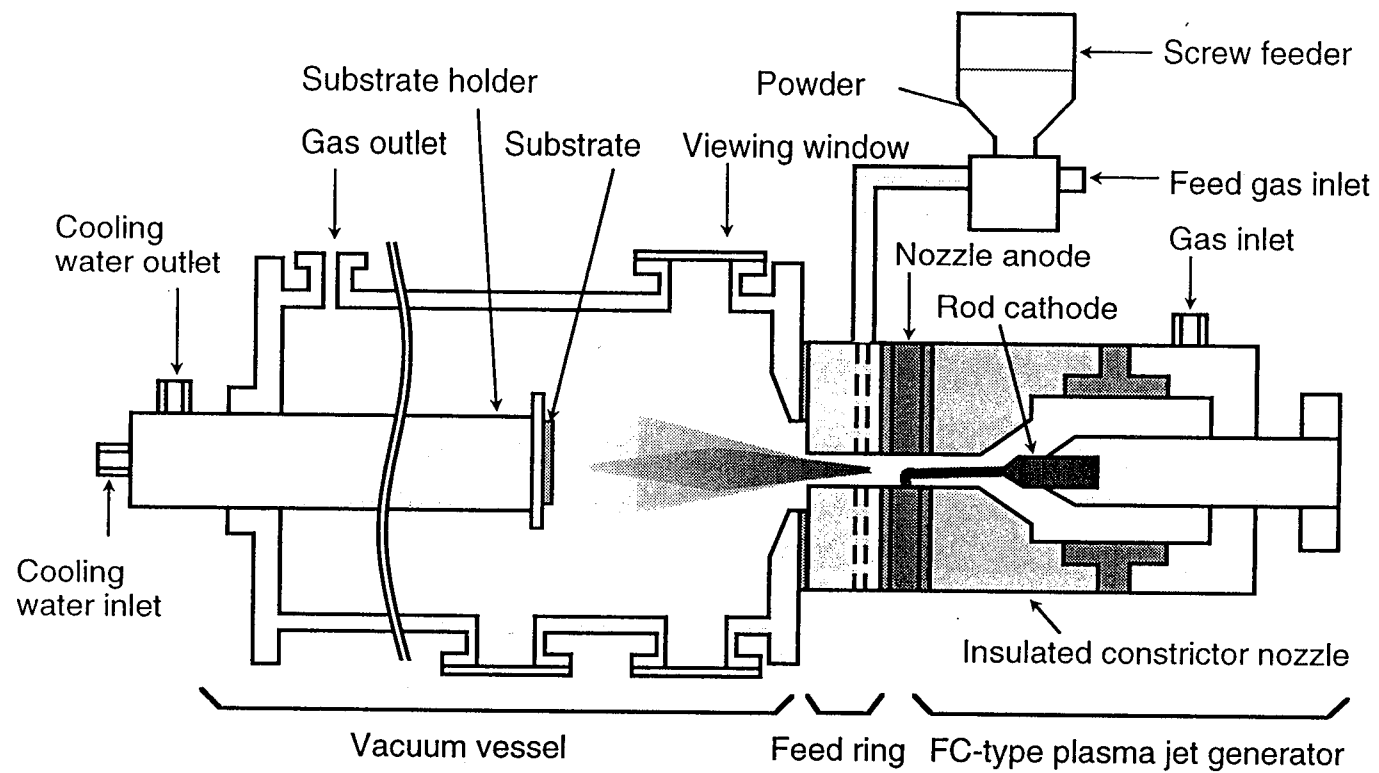


Fig.1

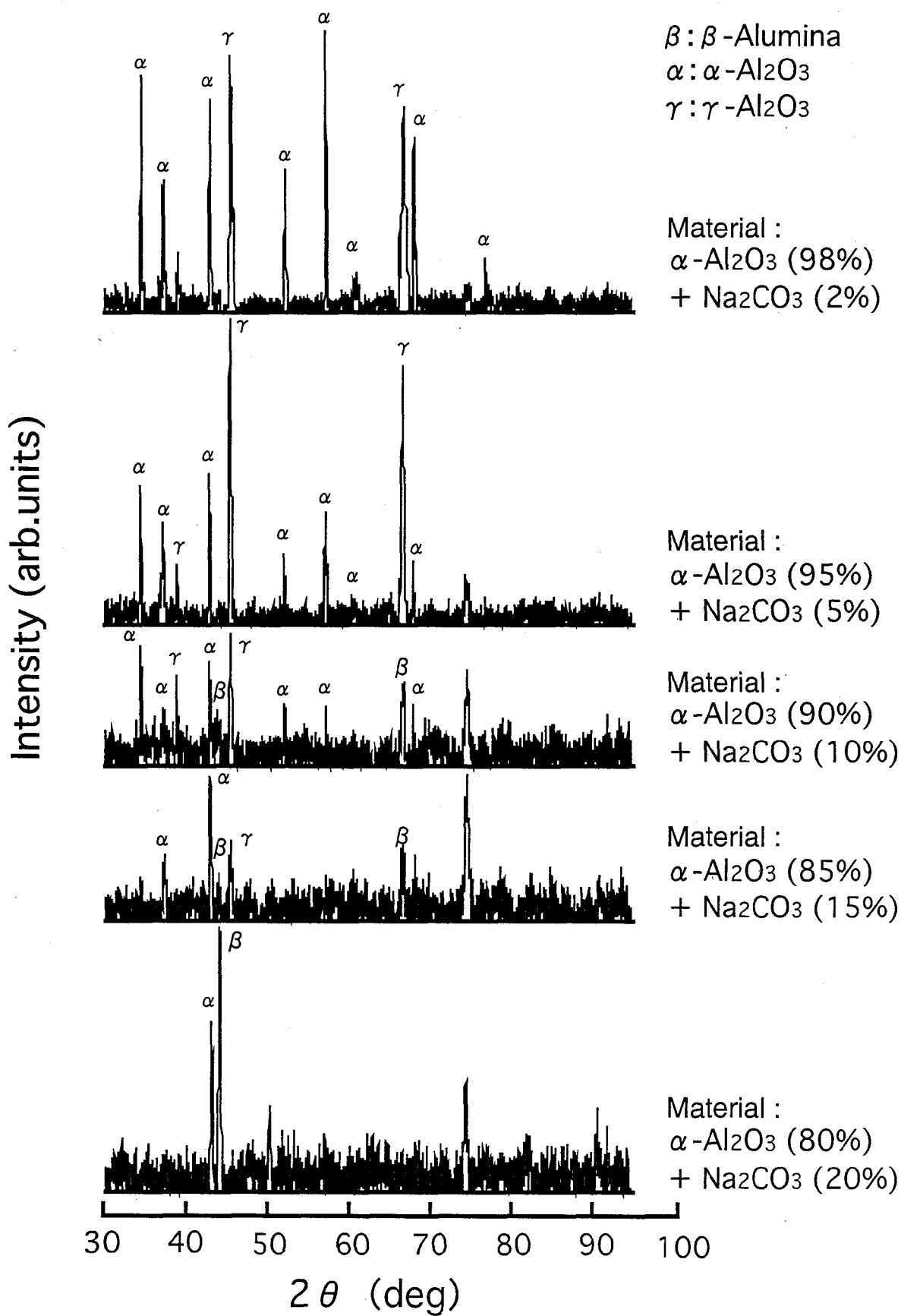


Fig.2

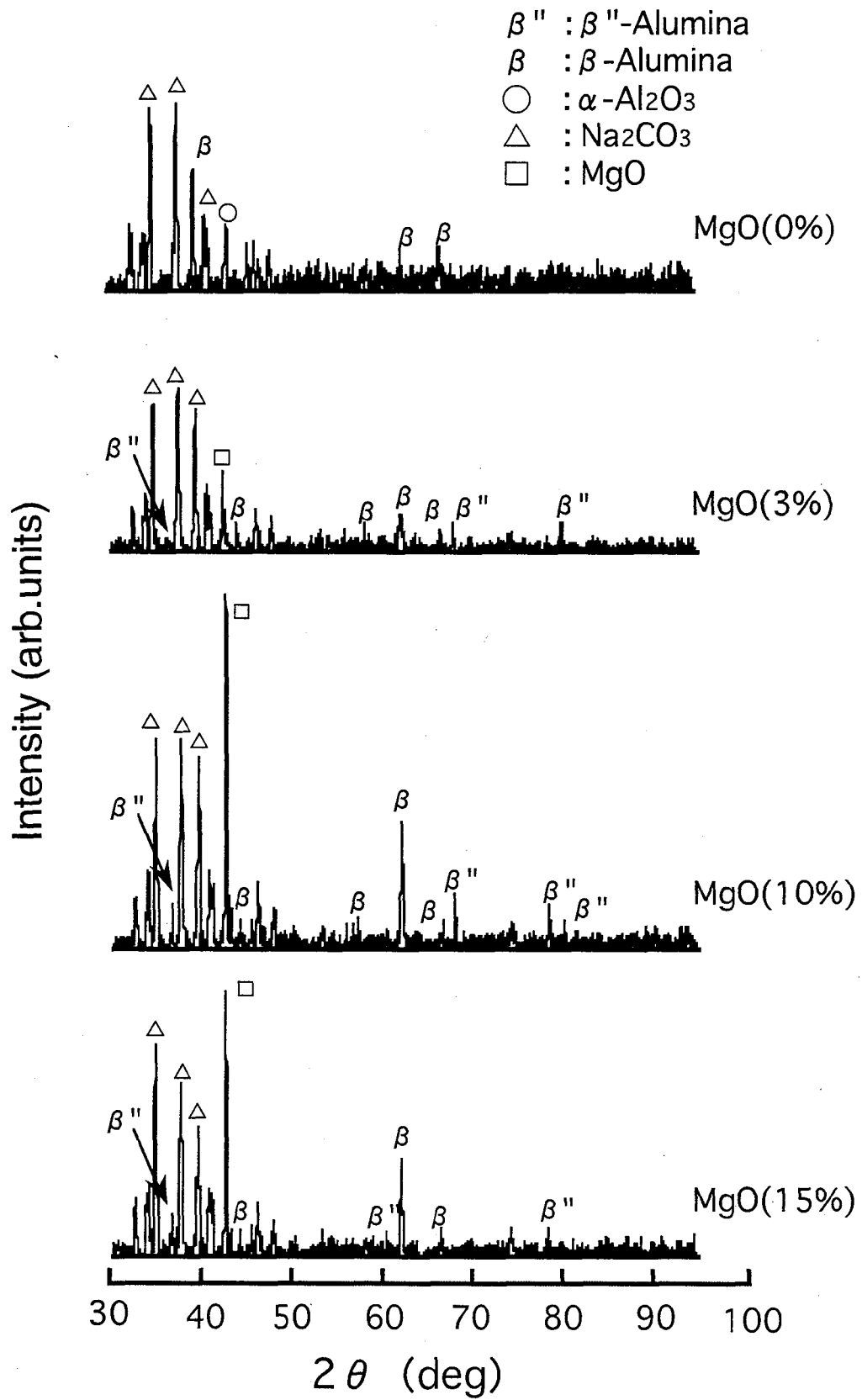


Fig.3

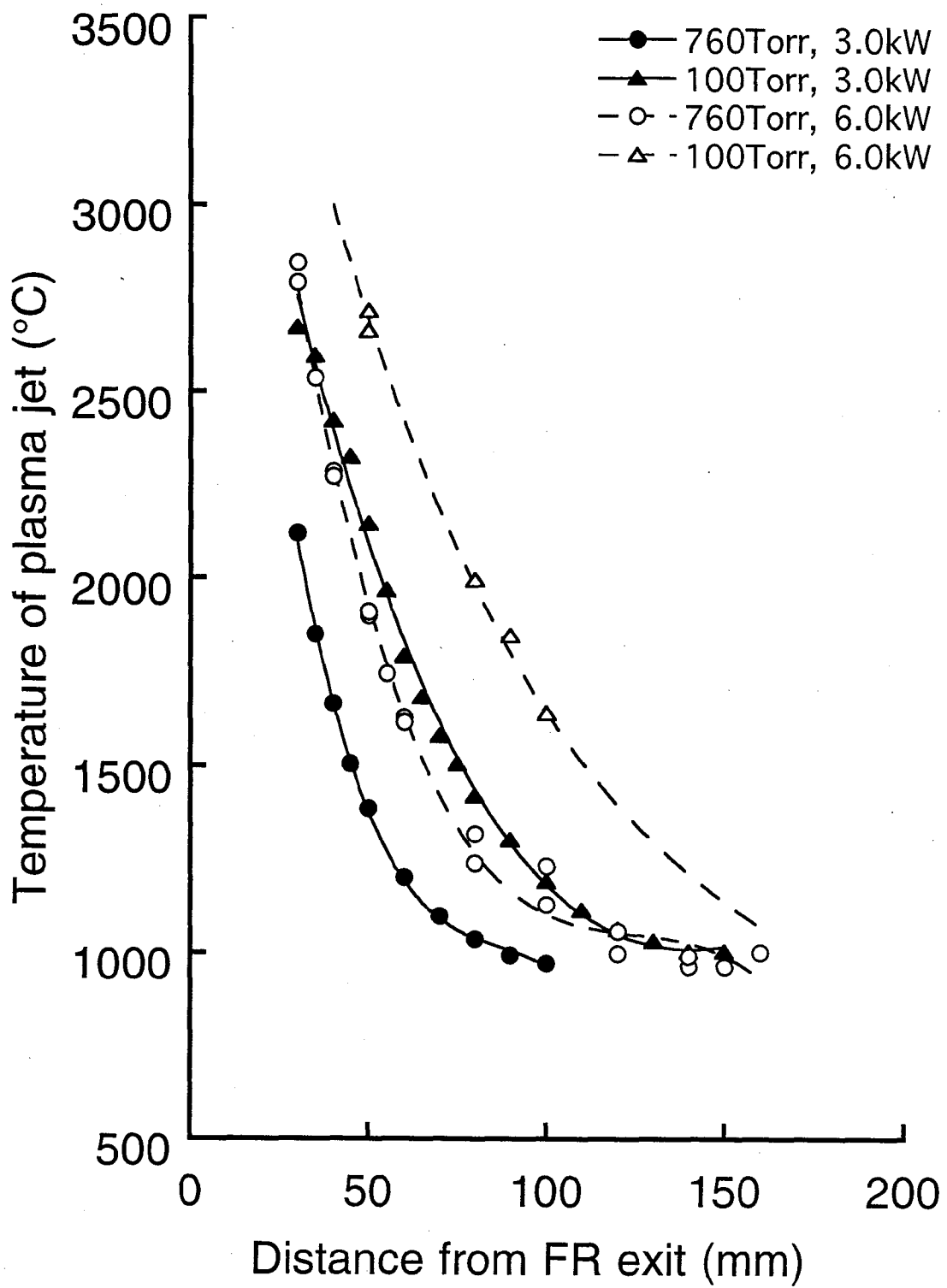


Fig.4

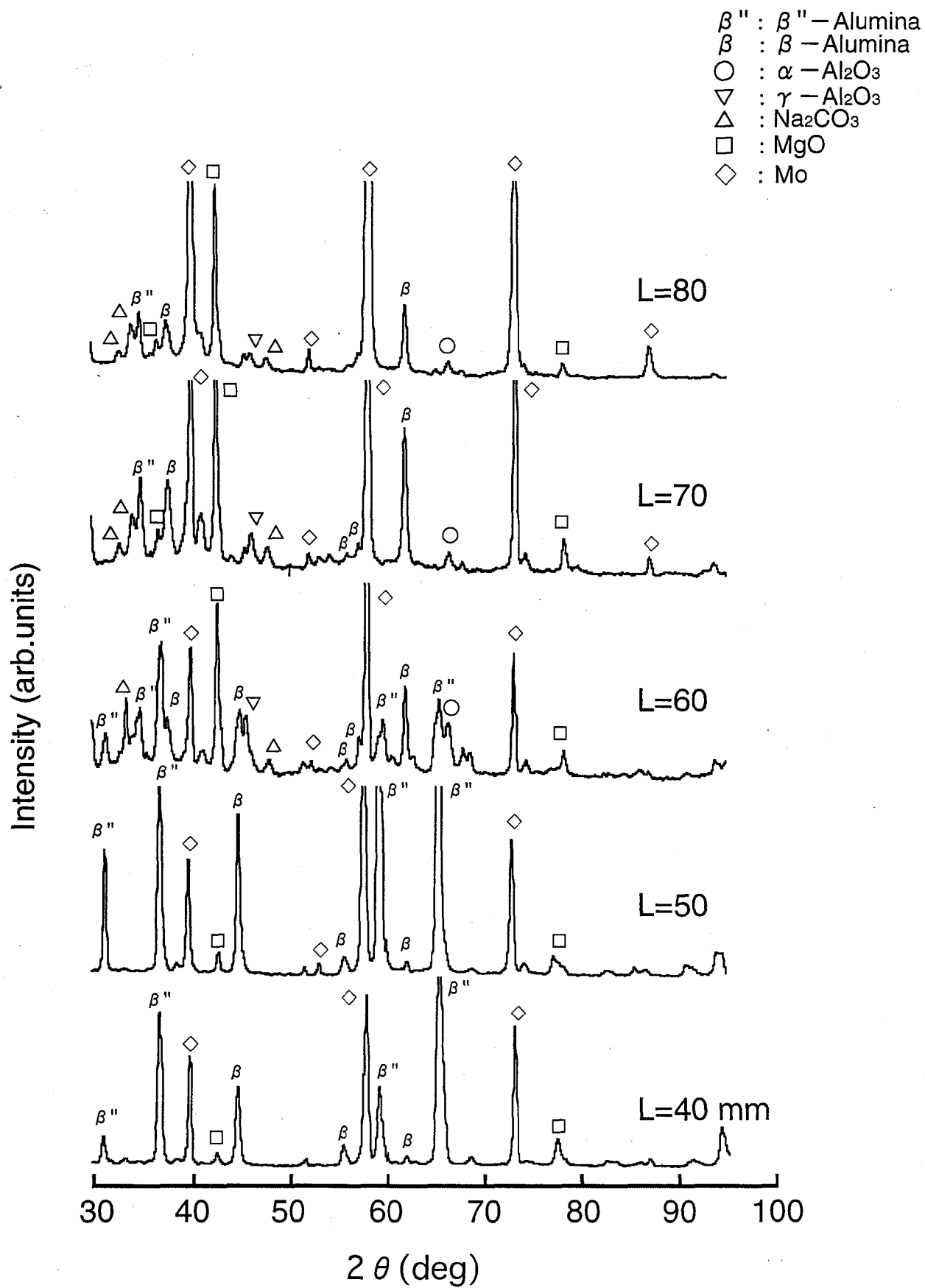
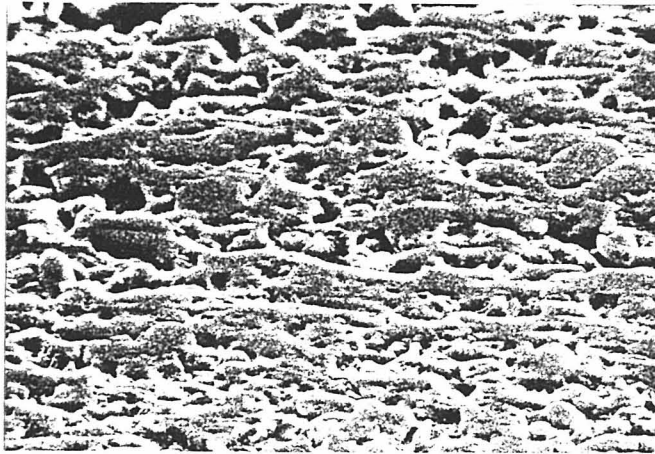
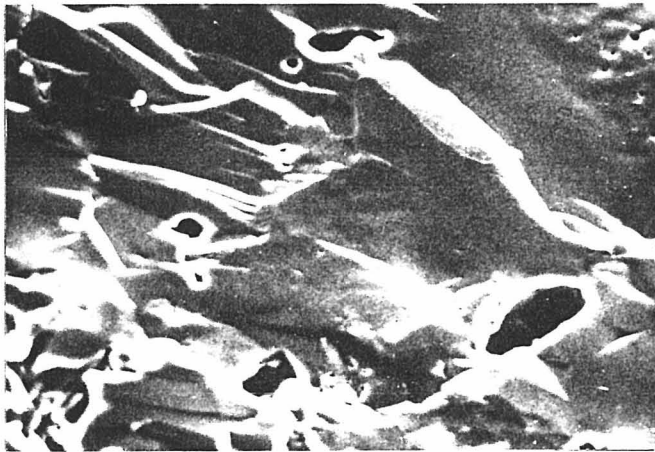


Fig.5

Cross-sectional view



50  $\mu$  m  
(a) L=80 mm



50  $\mu$  m  
(b) L=40 mm

Fig.6

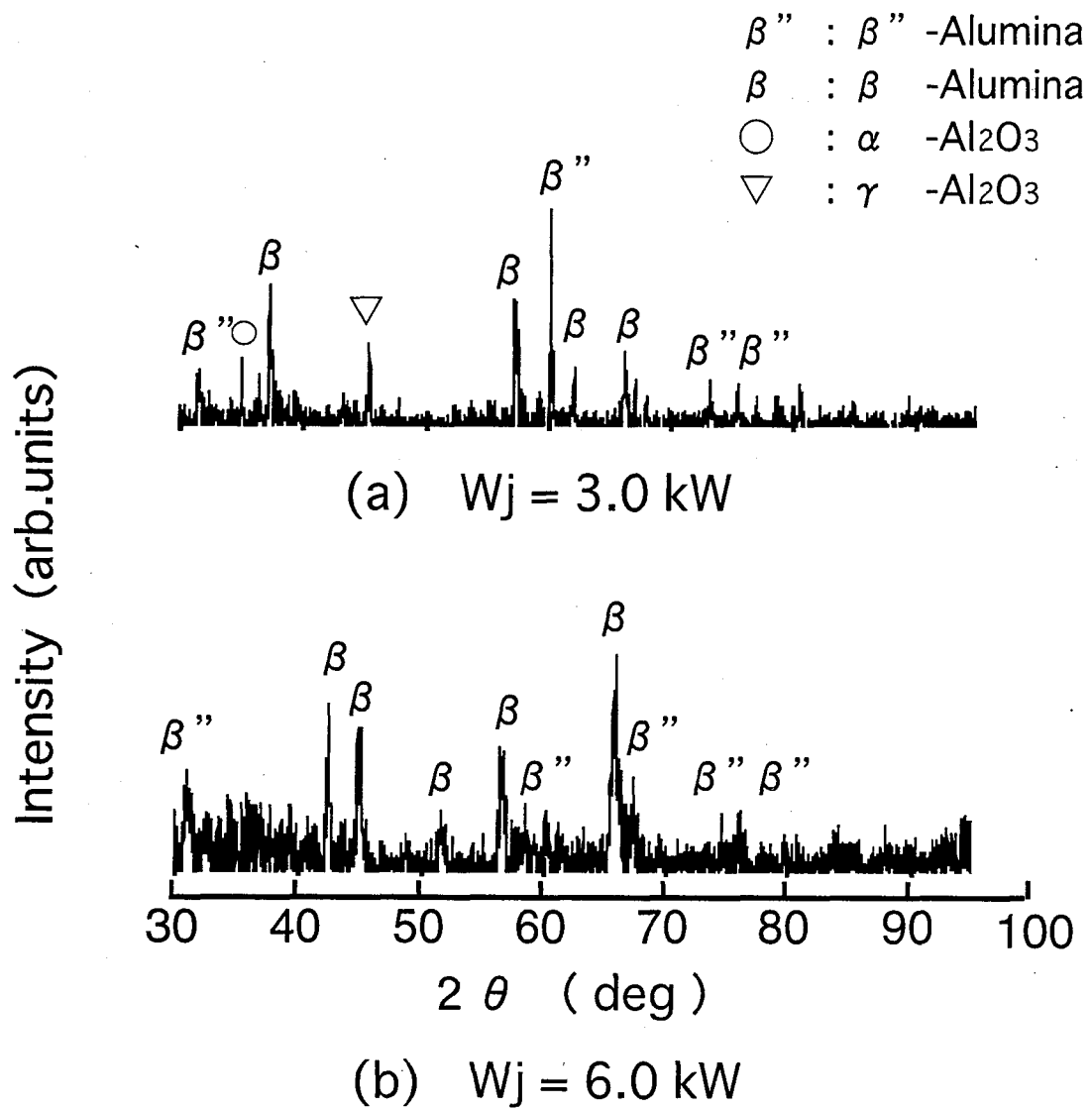


Fig.7



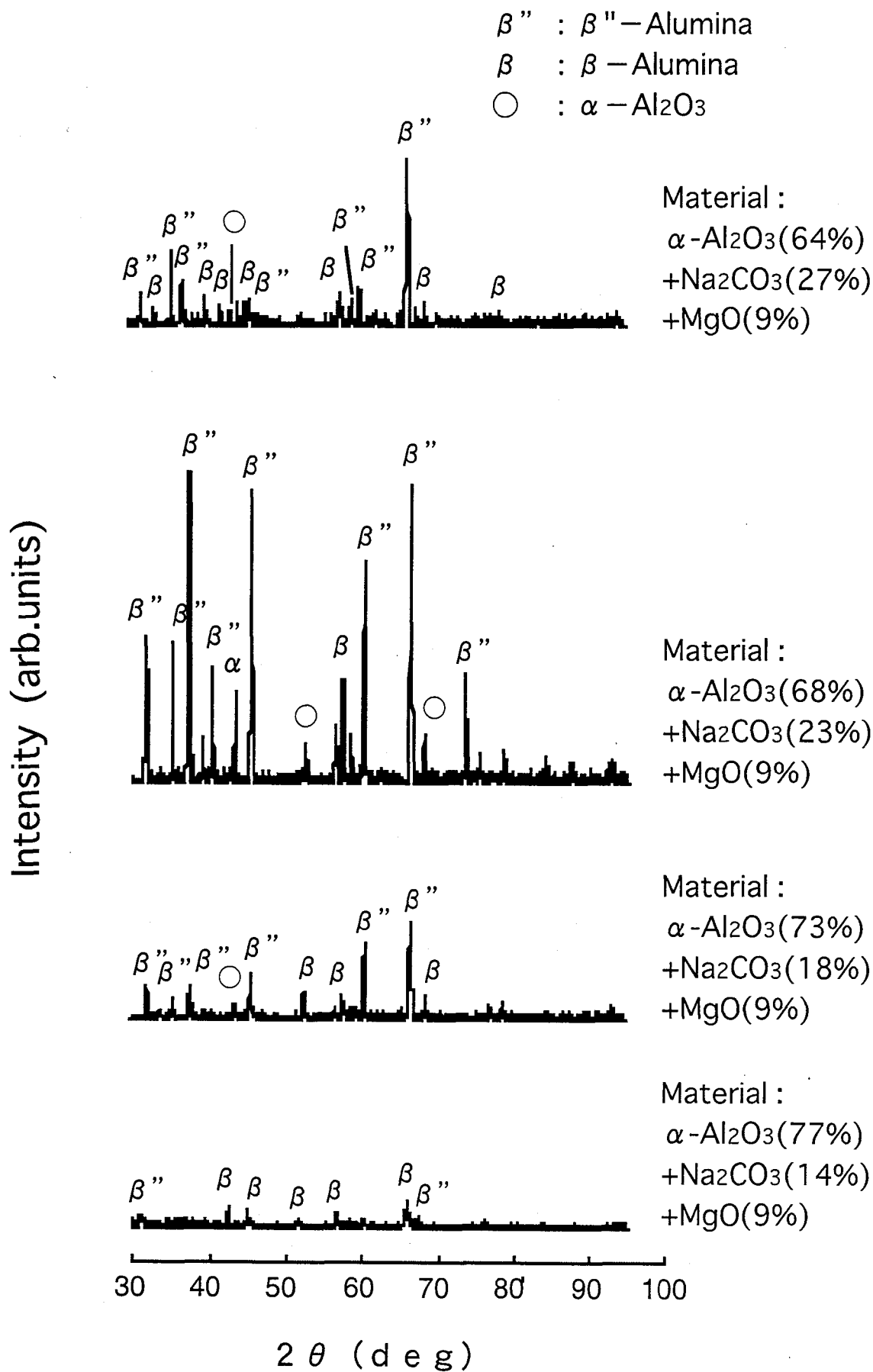


Fig.8